Acta Oceanol. Sin., 2020, Vol. 39, No. 5, P. 96–104
https://doi.org/10.1007/s13131-020-1571-7
http://www.hyxb.org.cn
E-mail: hyxbe@263.net

Wave flume experiments on dynamics of the bottom boundary layer in silty seabed

Mingzheng Wen[1, 2], Yonggang Jia[1, 3*], Zhenhao Wang[1, 4], Shaotong Zhang[1], Hongxian Shan[1, 3]

[1] Shandong Provincial Key Laboratory of Marine Environment and Geological Engineering, Ocean University of China, Qingdao 266100, China

[2] Tianjin Center, China Geological Survey, Tianjin 300170, China

[3] Laboratory for Marine Geology, Pilot National Laboratory for Marine Science and Technology (Qingdao), Qingdao 266061, China

[4] First Institute of Oceanography, Ministry of Natural Resources, Qingdao 266061, China

Received 10 June 2019; accepted 13 July 2019

Abstract

The objectives of this study are carried out a series of controlled large wave flume experiments using fine-grained sediment from the Huanghe River Delta, exploring the complete sequence of sediment behavior in the bottom boundary layer (BBL) during wave-induced liquefaction. The results show that: (1) The BBL in silty seabed is exposed to a progressive wave, goes through a number of different stages including compaction before liquefaction, sediment liquefaction, and compaction after liquefaction, which determines the range and thickness of BBL. (2) With the introduction of waves, first, the sediment surface has settled by an amount S (S=1–2 cm) in the course of wave loadings with an insufficient accumulation of pore water pressure. And a thin high concentration layer formed the near-bed bottom. (3) Once the liquefaction sets in, the liquefied sediment with an 'orbital motion' and the sub-liquefied sediment form a two-layer-sediment region. The range of BBL extends downwards and stopped at a certain depth, subsequently, develops upwards with the compaction process. Meanwhile, re-suspended sediments diffuse to the upper water column. (4) During the dynamics process of the BBL beneath progressive waves, the re-suspended sediment increment ranked as sediment liquefaction > erosion before liquefaction > compaction after liquefaction.

Key words: bottom boundary layer, suspended sediment concentration, liquefaction, compaction, Yellow River Delta

Citation: Wen Mingzheng, Jia Yonggang, Wang Zhenhao, Zhang Shaotong, Shan Hongxian. 2020. Wave flume experiments on dynamics of the bottom boundary layer in silty seabed. Acta Oceanologica Sinica, 39(5): 96–104, doi: 10.1007/s13131-020-1571-7

1 Introduction

The boundary layer is an important concept and refers to the layer of fluid in the immediate vicinity of a bounding surface where the effects of viscosity are significant. In marine geology, the bottom boundary layer (BBL) may be defined as the layer adjacent to the seabed in which the flow is affected by processes occurring at the boundary and in which strong gradients of physical, chemical, and biological properties may occur (Bowden, 1978). Previous reviews of the BBL in the ocean have focused primarily on the velocity field. An important aspect of a BBL is that the velocity of the fluid goes to zero at the boundary, at some distance above the boundary the velocity reaches a constant value. This is because the velocity shear in the BBL is particularly strong near the seafloor, and diminishes upwards, to become zero when approaching the ocean interior, where the velocity field is approximately constant and determined by the geostrophic balance. The thickness of the BBL depends on the influence of the seabed boundary on velocity, which is of the order of 10 m in the deep ocean (depths up to 4 000 m; Lueck et al., 2001), but under high-velocity current conditions, it may reach a thickness of 40 m (Kantha et al., 2000) or even involve the whole water column in shallow-water areas, where friction and currents are relatively strong compared to the deep ocean. Taking into account the exchange between the water column and sediment, the thickness of BBL could extend to a height of a few meters, or a few tens of meters above the seabed and it may also be said to extend a short distance of the order of centimeters or decimeters downwards into the sediment, since chemical properties in the water column are continuous with those in the pore water of the sediments and the processes of erosion, deposition, and bed movement of material involve both sides of the water/sediment interface (Bowden, 1978). McKee et al. (2004) pointed outthat the BBL to encompass the region 1 to 2 m above the sediment/water interface and the mobile upper region of the seabed (including fluid muds and ephemeral surface sediments).

It is well recognized that the hydrodynamic properties of the BBL affect sediment resuspension. The shear stress near the bed directly causes sediment erosion, affects vertical mixing, and relates to conditions conducive to sediment deposition. Considering the condition of sediment availability or supply, it may re-

Foundation item: The National Natural Science Foundation of China under contract Nos 41427803 and 41807229; the Joint Fund of NSFC and Marine Science Research Centers of Shandong Province of China under contract No. U1606401; China Geological Survey Program under contract No. 121201006000182401.

*Corresponding author, E-mail: yonggang@ouc.edu.cn

late to micro-scale sediment mixing, such as flocculation and hindered settling (Hir et al., 2000); it could form a stepped vertical profile of suspended sediment concentration (SSC) and trap sediment in the near-bed layer. The BBL can be subdivided into four regions (Fig. 1), according to the bulk density and concentration of suspended sediment: (1) Low-concentrated layer, alias dilute suspensions. These suspensions were considered to be dilute non-interaction, and Newtonian suspensions (Chang et al., 2012; Bruens, 2003). (2) High-concentrated layer, also known as concentrated benthic suspensions, which is defined as a suspension of cohesive sediment with a notable interaction between the sediment and the turbulent flow field through buoyancy effects, but still displaying near-Newtonian behavior (Winterwerp et al., 2002). (3) Fluid mud (Hyper-concentrated benthic layer). In general, fluid mud is considered a high-concentration sediment suspension, here taken to be sediment suspensions with mass concentrations >10 g/L and <400 g/L (Ingliss and Allen, 1957; Krone, 1962; Wells, 1983; Ross, 1988; Kineke et al., 1996). Fluid mud is not considered part of the consolidated seabed because it lacks mechanical strength; it can be mobile (Bingham Fluids) or stationary above the stable seabed and can significantly modify the transporting flow. (4) Liquefied or underconsolidated bed, which could be considered part of the consolidated seabed, and the seabed sediments may become unstable or even liquefied induced by gravity forces and storms. Once liquefaction occurs, the sediment particles are likely to be carried away as a fluid by any prevailing bottom currents or mass transport (Jeng, 2001).

The Huanghe River is well known for its high sediment concentration, the suspended sediments of the Huanghe River are derived from the loess plateau where the sediment is loose and easily eroded by storms. The grain size of suspended sediments is finer in the Huanghe River Delta. The sediment transportation, fluid, liquefaction, instability characteristics in the Huanghe River Delta have been observed and studied for the last 40 years (Prior et al., 1986; Van Den Berg and Gelder, 1993; Wei et al., 1995; Jia et al., 2014; Wang et al., 2014; Xu et al., 2016; Zhang et al., 2018a, b). The shallow surface sediments of silty sediment seabed in the subaqueous Delta of the Huanghe River estuary are often liquefied or partially liquefied owing to the action of ocean waves, which lead to the initially consolidated seabed from the solid phase to liquid phase and a part of the BBL. In liquefaction studies of the seabed sediment in the Huanghe River Delta, the liquefaction depth, in 8 m of water, could reach 4.1 m, and collapses occurred in the liquefied seabed (Sun et al., 2008; Xu et al., 2008). Under ocean waves, dynamic bottom pressure fluctuation on a compressible silty seabed and pore pressure build-up might exceed the overburden, which destroyed the original consolidated sediment granular skeleton, increased the permeability of the seabed (Mörz et al., 2007) weaken a seabed strength, thus inducing seabed fluidization (Sumer et al., 2006; Jeng, 2013). On the other hand, wave-induced pore pressure build-ups have significant promoting effects on the concentration of suspended substances (Jia et al., 2014; Guo et al., 2016; Zhang et al., 2018a). Thus liquefaction induced by wave plays an important role in the dynamics of the BBL. The objectives of this study are carried out a series of controlled large wave flume experiments using fine-grained sediment from the Huanghe River Delta, exploring the complete sequence of sediment behavior in the BBL during wave-induced liquefaction including excess pore-water pressure buildup, distribution of sediment resuspension concentration in the water column.

2 Experimental methodology

The experiments were carried out in an indoor wave flume, which is in the Geotechnical Laboratory, Ocean University of China. Regular waves were produced by a piston-type wave generator. The water depth was maintained at 40 cm.

2.1 *Instruments and equipment*

A sketch of the wave flume is shown in Fig. 2. The wave flume was approximately 14 m in length, 0.5 m in width and 0.7 m in depth. It is equipped with a piston-tape wave generator on the

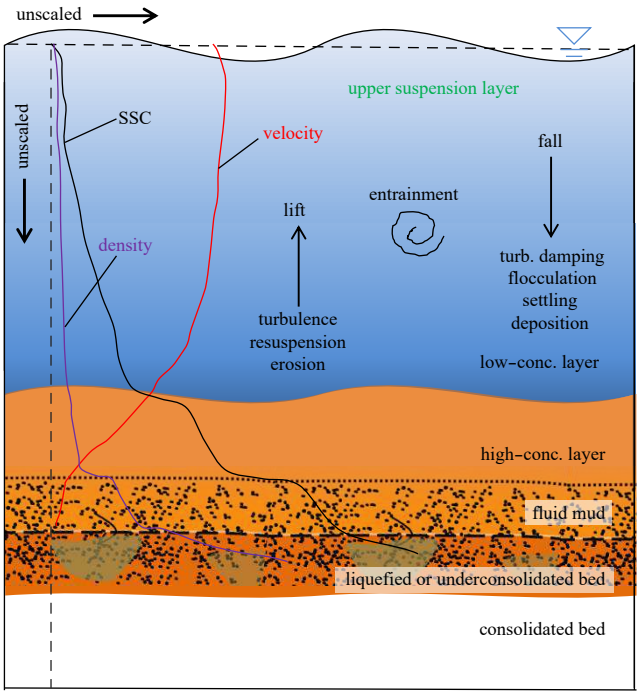

SSC/kg·m^{-3}	Bulk density/kg·m^{-3}	Fluid behavior
<10	1 000–1 020	newtonian
1 to several 10 s	1 020–1 050	newtonian
several 10 s to a few 100 s	1 050–1 300	bingham
transition	transition	–
> 750	>1 300	solid-state

Fig. 1. Perspectives on the dynamics of the bottom boundary layer in the water column (SSC is suspended sediment concentration, layer thickness is not to scale) (Refer to Wan et al., 2014).

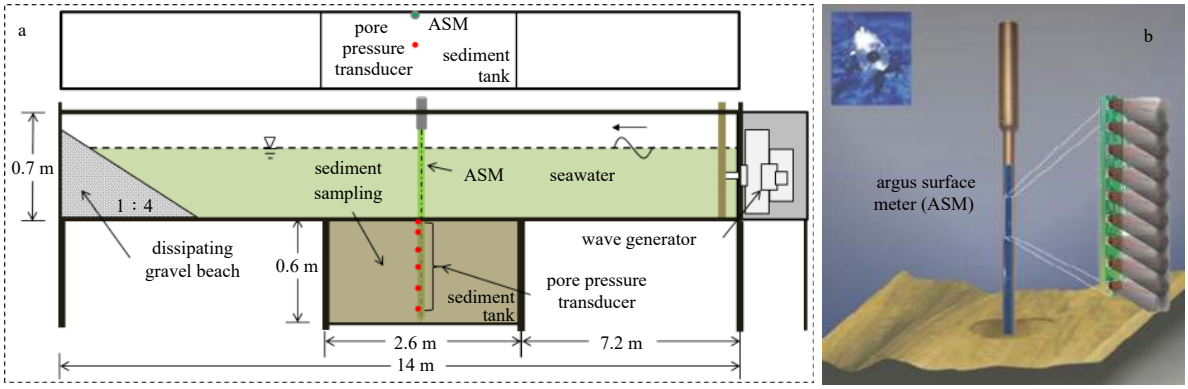

Fig. 2. Set-up of the indoor wave flume. The wave generator is located at the right end of the water flume, and the wave absorber is located at the left end. Argus surface meter, the instrument operates with a series of backscatter infrared sensors (spaced at 10 mm) that are embedded in intervals in a solid pile made of stainless steel.

one end, and a 1:4 dissipating gravel beach on the other end. A glass-walled sediment tank (2.6 m (L)×0.6 m (H)×0.5 m (W)) embedded in the wave flume filled with sediment, the transparent sidewalls of the sediment tank provided convenience for us to observe the phenomenon of the sediment responses under wave action. Regular water waves were paraded from one side of the flume and disappeared when the front waves reach the dissipation system, and wave parameters can be changed by controlling the driving frequency (Jia et al., 2014; Zhang et al., 2018b).

The pore-water pressure measurements were performed via six pore-water pressure transducers (CYY2, China, 5 mm in diameter and 12 mm in length, with 1 Hz, continuous) which deployed along the central site of the sediment tank at six different depths, Z=7, 12, 20, 28, 36 and 44 cm, in which Z is the vertical distance measured downwards from the initial seabed surface. The spatial and temporal changes of suspended sediment concentration (SSC) in the water column were records via an Argus Surface Meter IV (ASM, Argus, Germany, with frequency 1 Hz, 10 min interval), ASM is a high-resolution SSC profiler and operates with optical backscatter infrared sensors (OBS) embedded in a stainless steel rod, the sensors are placed on an active board at a distance of 10 mm. The ASM records the reflections and the dynamic parameters that are created in the water column by solid particles moving in a multiphase current, and responds directly to SSC's and thus may be used to identify process-driven variations in water turbidity. The conversion from signal reflectivity (R_s, FTU) to SSC values has been achieved using a calibration function defined in the laboratory prior to field deployment, further descriptions of the calibration methodology can be found in Guo et al. (2016). The signal reflectivity to suspended sediment concentration conversion formula was deduced via linear regression (Fig. 3). As R^2 was 0.955 3, which indicates that the conversion is reliable enough to estimate the SSC with accuracy.

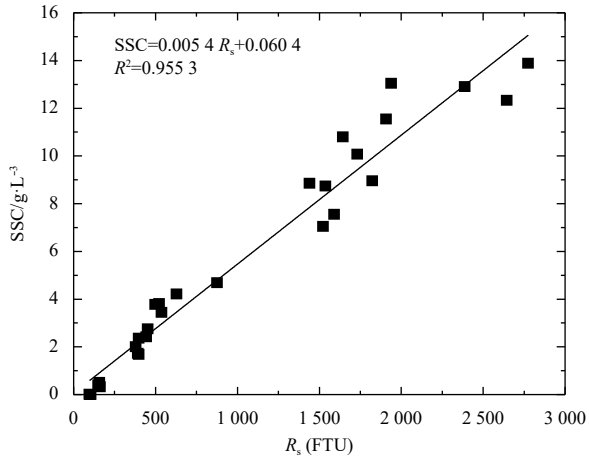

Fig. 3. Conversion formula from signal reflectivity to SSC derived from the calibration experiment.

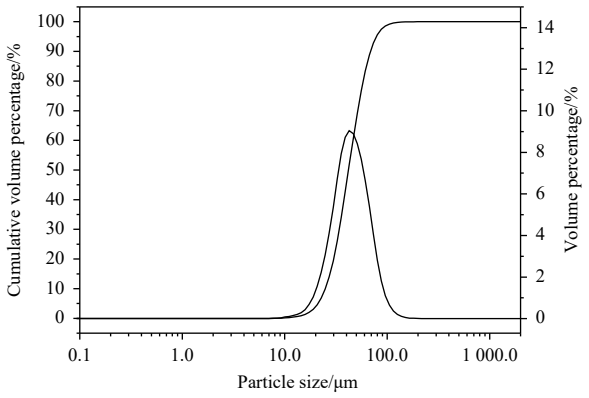

Fig. 4. Grain-size distribution of the initial sediment bed.

2.2 *Sediment and test conditions*

The sediment used in the experiment was from the tidal flats of the subaqueous Huanghe River Delta. The sediment was silt with D_{50}=43.04 μm and the geometric standard deviation is $\sigma_g(=\sqrt{d_{84}/d_{16}})$ = 1.5. The particle size distribution (PSD) is given in Fig. 4. The PSD curve was determined using the Rise-2002 mode laser Particle analyzer. The sediment properties are given in Table 1. In the table, γ is the specific weight of sediment and w is the water content. Other quantities are described in the table. Before the experiment, air-dried sediment was crushed and thoroughly mixed with water and homogenized to make saturated slurry, which was used as the initial seabed. In the sediment tank, the initial sediment depth was 62 cm. A week later, the seabed sediments were consolidation by drainage, and then the depth of seabed sediments was reduced to 60 cm. The properties of sediment for initial seabed were summarized in Table 1.

2.3 *Quantification of the re-suspended sediment*

According to the distribution curves of background SSC and SSC under wave loading, the net re-suspended sediment concen-

Table 1. The properties of initial seabed sediments used in the experiment

Unit weight γ/kN·m^{-2}	Water content w/%	Void ratio e	Specific gravity[1)] G_s	Grain size		
				D_{10}/μm	D_{50}/μm	D_{90}/μm
18.2	32.0	0.92	2.70	26.22	43.04	69.97

Note: [1)] Specific gravity referred to the result of the experiment of Liu et al. (2016).

tration can be calculated, which represented the amount of sediment transferred from underneath the sediment bed into the water. The net re-suspended sediment ($Q_{\rm net}$) per basal area water column was adopted as an index representing the variability net re-suspended sediment, which can be calculated by the following formula (stratified summation method):

$$Q_{\rm net} = \int_0^h C_{\rm net}{\rm d}z \approx \sum_{i=1}^{n} (C_i - C_{bi}) \times h_i. \quad (1)$$

The basic assumption of the stratified summation method is that SSC at the same elevation in the water flume can be represented by the reference concentration of the data from ASM, the concentration of this water layer is assumed to be horizontally uniform. $Q_{\rm net}$ denotes the quantity of re-suspended sediment within a unit basal area water column (kg/m^2); i is the partitioning layer number in the water column; and h_i=1 cm represents the thickness of each layer (depends on the distance between sensors of ASM), and n= 31 (regardless of the effects of sea-bed interface changes and sea level fluctuations). $C_{{\rm net}i}$=C_i–C_{bi} is the net re-suspended sediment concentration of each layer, the C_i and C_{bi} represent the instantaneous SSC and the background SSC of each layer.

2.4 *Experiment procedure*

Four designed wave conditions (with a wave height of 6, 10, 14 and 18 cm respectively) were successively loaded on the seabed until the SSC finally attain an equilibrium state. The wave parameters were summarized in Table 2. In the table, h is the depth of water, H is wave heights, T is the wave period and L is the wavelength, $T_{\rm dw}$ is the duration of wave action. In the test, liquefaction of sediment or not was discriminated by observing the oscillatory motion of the sediment. During the experiments, the ASM was used to measure the turbidity of the water in predetermined time intervals (Period of a single measurement: 10 s). The variation of pore water pressure is recorded by pore-water pressure transducers. The experimental phenomena including: (1) the time development of the sediment/water interface, (2) the time development of the liquefaction front, (3) the time development of the compaction front, and (4) the characteristics of the liquefied sediment oscillation were recorded by video camera.

Table 2. Summary of flume experimental conditions

Test series	h/cm	H/cm	T/s	L/m	Liquefaction	$T_{\rm dw}$/h
1	40	6	2.42	4.57	not	1.5
2	40	10	1.30	2.17	not	3.0
3	40	14	1.02	1.51	not	1.0
4	40	18	1.35	2.28	yes	18.0

3 Results

3.1 *Experimental phenomena*

Over the course of the experiments, typical photographs were arranged orderly in Fig. 5, in which the first (Fig. 5a) is a consolidation period during which the pore water and bubbles flow up to the seabed surface, resulting in the formation of micro-mud volcanoes. The wave column is clear due to the lack of wave loading; Fig. 5b is the response of seabed during the initial period of 6 cm wave action, during which no significant movement of sub-bottom sediments was detected, which indicates that there is no liquefaction in the seabed. Surface sediments moved along the sediment/water interface, and the water column gradually became too turbid to identify the interface. There was also no signi-

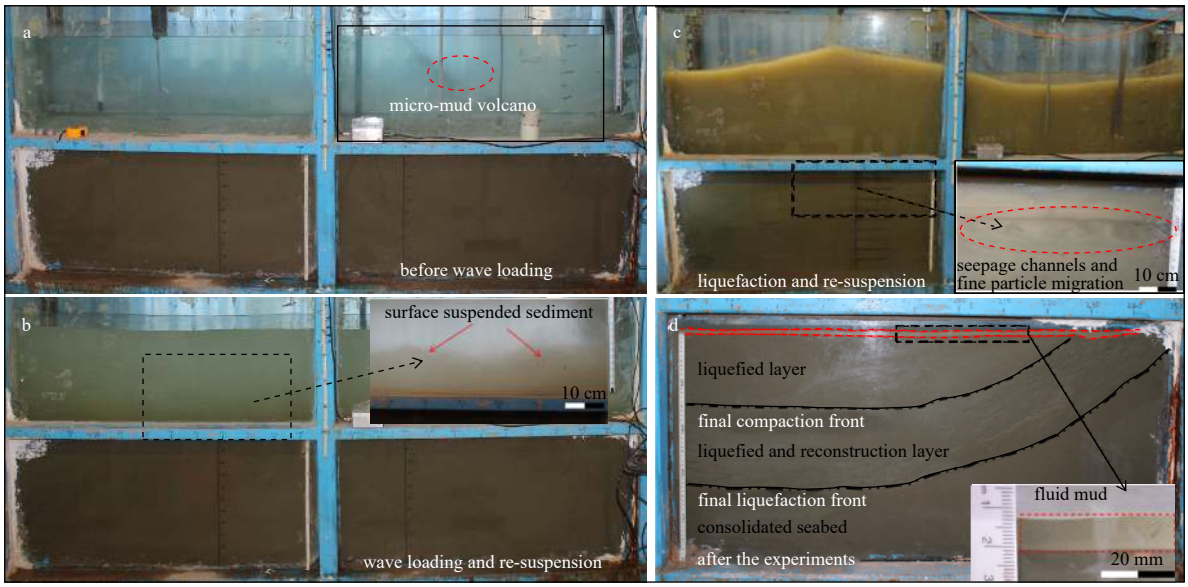

Fig. 5. Typical photographs of the characteristics of seabed responses to waves during the flume experiment and the resulting features. a. In a consolidation period before wave action which micro-mud volcanoes appeared on the seabed surface; b. the initial period of 6 cm wave action, surface sediments moved along the sediment/water interface and spread to upper water column; c. under 18 cm wave loading, during which seepage channels were observed; d. typical stratification characteristics of seabed sediment after wave termination.

ficant movement of sub-bottom sediments during the 10 cm, 14 cm wave action, but the more surface sediments move into the water column; Fig. 3c is the response of seabed during the period of 18 cm wave action, the seepage channels were observed and the sub-bottom fine particle migration up to the seabed surface. The experiments of Liu et al. (2017) and Xu et al. (2016) were also conducted in the same wave flume using similar Yellow River silts, and similar experimental phenomena were found in these experiments. Subsequently, a partial liquefaction zone formed in the shallow layers, the sediments began to oscillate horizontally along an arc-shaped sub-bottom sliding interface. Meanwhile, sediments were re-suspended again until a liquid of higher turbidity; and Fig. 5d is the typical stratification characteristics of seabed sediment after the termination of waves. The liquefaction front traveled downwards under the action of wave loading and the liquefied areas developed over time in both horizontal and vertical directions. Finally, the liquefaction front stopped at a certain depth, and then the compaction process began from the bottom of the liquefied zone, the compaction front moved upwards, compaction front also stopped at a certain depth (Maybe, the compaction front could arrive at the surface of the sediment, if the time is long enough, or the wave energy decreases). The superficial sediments, which located between compaction front and the sediment/water interface kept oscillating elliptically with waves. A fluid mud layer formed on the surface of the seabed after wave termination due to re-settled of re-suspended sediments in the water column.

3.2 *Liquefaction*

In order to judge the occurrence of the liquefaction, the wave-induced pore pressure responses to waves at 12, 20, 36 and 44 cm below the initial sediment/water interface during the corresponding period are presented in Fig. 6a. However, no reliable results were obtained due to some unknown problems of the pore-water pressure transducers located at 7 and 28 cm below the initial sediment/water interface. During the period of 6, 10 and 14 cm wave actions, the pore pressure started to fluctuate and accumulate when the subsequent waves were switched on. After that, the accumulated pore pressure (excess pore pressure) dissipated with the duration of wave loading. There was no significant movement of sub-bottom sediments was detected. When t=330 min, the 18 cm waves were switched on and the then pore pressure built up in a short period to offset overlying effective stress, liquefies the seabed and dissipates over a longer time subsequently.

This wave-induced liquefaction process has been studied independently in similar experiments (e.g., Jia et al., 2014; Xu et al., 2016; Liu et al., 2017), in the present authors, the most representative phenomenon of seabed liquefaction in the wave flume is the elliptical motion of sediments with the wave. The “elliptical motion of sediments” as a sign of liquefaction is used herein. After sediment liquefaction, a liquefaction zone formed in the shallow layers and subsequently spreads downwards (Fig. 6b). In the initial stage, the liquefaction in depth expanded rapidly. After reaching 39 cm (the value is 27 cm in the experiment of Xu et al.

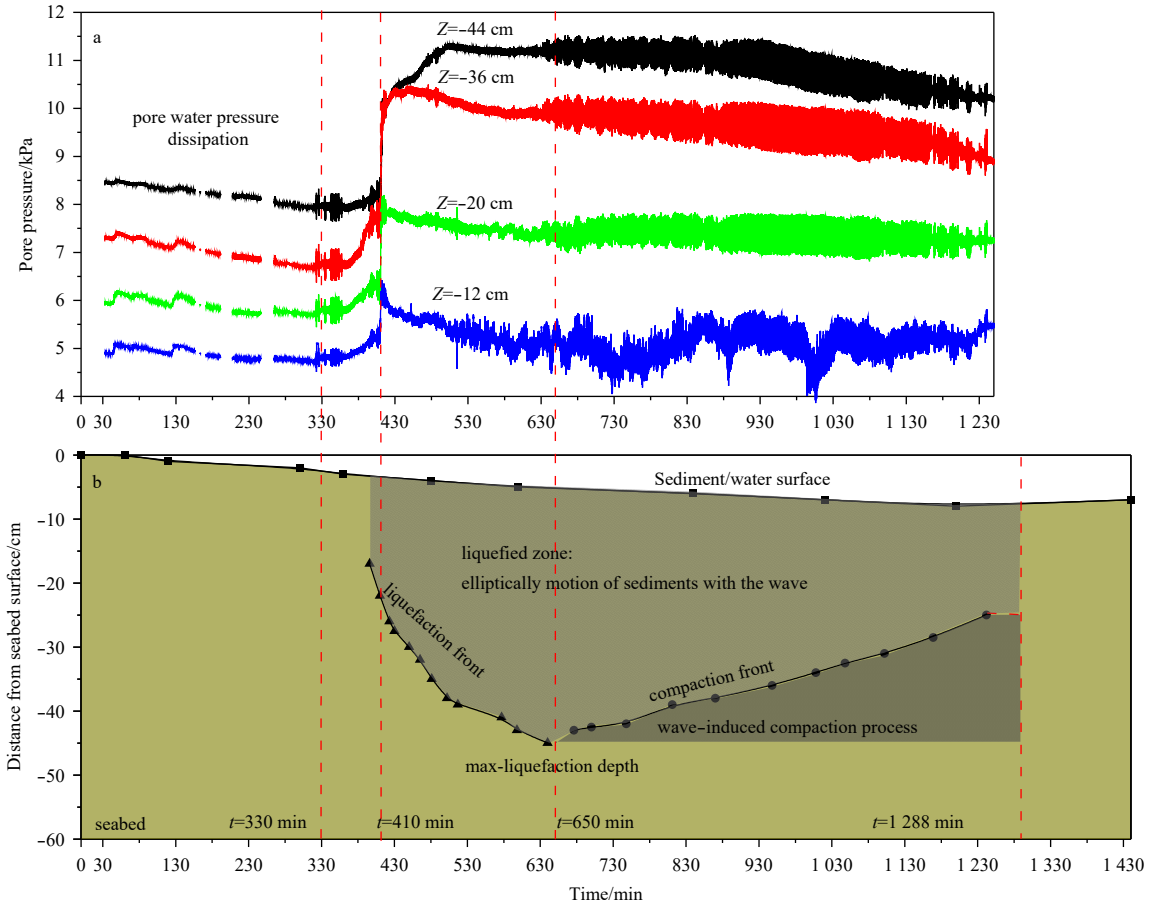

Fig. 6. The response of sediment under wave actions. a. Pore pressure responses at various observation depths (12, 20, 36, and 44 cm) below the initial sediment/water interface; and b. time series of initial sediment/water interface, liquefaction front, and compaction front. t=0 min, began to wave loads; t=330 min, began to 18 cm wave action; t=410 min, a sharp increase of pore water pressure; t=650 min, liquefaction front reached the maximum depth.

(2016)), variation in liquefaction depth began to decrease. At t=650 min, the liquefaction front reached a limit liquefaction depth of 45 cm. After that, the latter process gradually progresses in the upward direction. The process resembles the self-weight consolidation of hydraulic fill although, which the waves continue during the process. Miyamoto et al. (2004) termed the process "solidification process" and Sumer et al. (2004) called it "compaction process". The latter term is used herein, as it refers to compaction of sediment by waves, an expression frequently used in hydraulic/coastal engineering practice.

With the sediment liquefied, there are two distinct layers of sediment: one with a distinct "orbital motion" of sediment with waves (the top layer is in the liquefied state), and the other with no orbital motion at all (the bottom layer) which is in the solid-state with the interface between the two layers (the compaction front) moving gradually in the upward direction. With the wave action, the speed of upward movement of the compaction front was significantly less than the speed of downward movement of liquefaction front, and the compaction front stopped at 25 cm below the initial sediment/water interface, finally. At any time, the water column and the liquefied sediment also formed a two-layered system of liquids (of different density) (discussed later).

3.3 *Time profiles of SSC*

The response of SSC under wave actions is divided into five processes (as shown in Fig. 7). Stage Ⅰ: The consolidation period, no wave loading. The SSC of the water column was close to 0.5–0.7 g/L in this period, as shown in Fig. 5a, the water column was clear and transparent. Stage Ⅱ: The responses of SSC during the period of 6, 10, 14 and18 cm wave actions. Obviously, waves mobilize sediments on the bed, distribute them vertically in the water column to produce a net suspension of sediment grains.

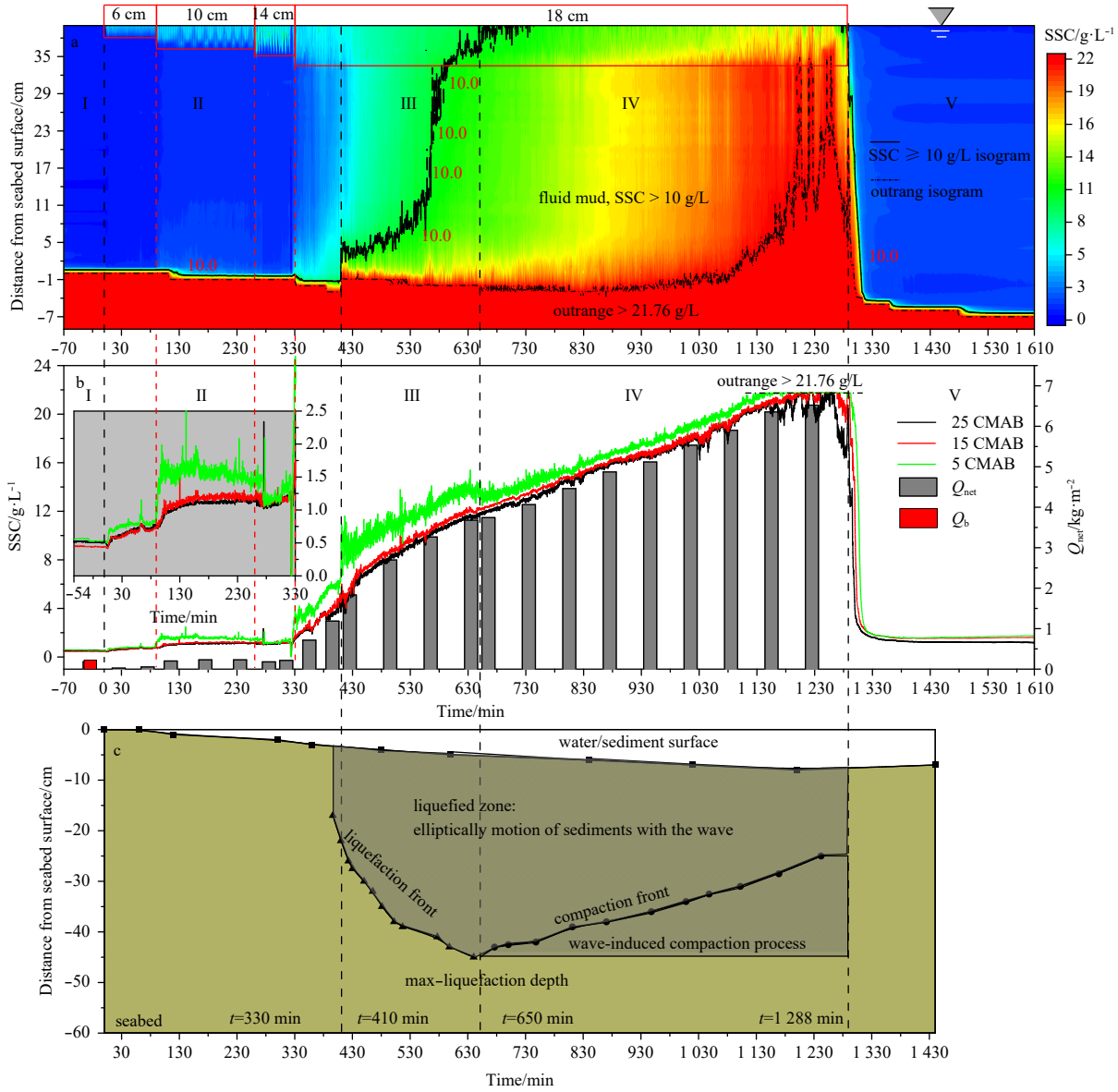

Fig. 7. The response of SSC under wave actions. a. Time-space diagram of SSC during the experiment, where black solid line is the isogram of SSC⩾10 g/L, short dash-dot represents the water/sediment interface before the onset of liquefaction (t<410 min) and indicates the data beyond the range of ASM in the water column (t⩾410 min); b. the time series of SSC at the depths of 5, 15, and 25 centimeters above the bottom (CMAB) and the net re-suspended sediment (Q_{net}) per basal area water column (Q_b represents the background suspend sediment per basal area water column); and c. same as Fig. 6b.

The SSC of the water column would finally attain an equilibrium state if the wave lasts long enough, such as the period of 10 cm wave loads. The re-suspended sediments formed a high-concentration layer, the thickness is less than 5 CMAB (centimeters above the bottom) and SSC < 2 g/L. The fluid mud layer (SSC > 10 g/L) with a thickness of about 1.0 cm was formed, and the thickness of it is more than 2.0 cm under the 18 cm wave loading. The sediments under water/sediment interface did not have absolute movement and only surface sediment erosion. Stage Ⅲ: The onset of liquefaction and the liquefied zone extended downward. At this stage, more sediments were suspended into the water column and constantly dissipated upwards along with the downward expansion of the liquefaction front. As a result, the thickness of the fluid rapidly extended to the whole water column. And a sharp increase was observed of the net re-suspended sediment (Q_{net}) per basal area water column after the onset of liquefaction. Stage Ⅳ: Compaction process, developed at the base of the liquefied sediment layer. The liquefaction front came to a standstill at a certain sediment depth. Under the further continuation of wave loads, the compaction began to develop. In the process of consolidation, the SSC and Q_{net} increased continuously and the SSC of water column exceeded the maximum range of the instrument. Stage Ⅴ: Re-settlement of suspended sediment without wave loads. At the end of the experiment, the wave load was stopped. Subsequently, the elliptical movement of shallow sediments stopped and the suspended sediments rapid settled.

4 Discussion

4.1 *Progressive evolution of BBL in sediments*

As mentioned previously, the progressive evolution process of BBL in this experiment can be divided into five subphases according to the response of seabed sediment under wave actions. Consider sinusoidal wave trains propagate over a level bed. The passage of wave trains induces an oscillation in the fluid pressure acting on the sediment bed. The wave pressure oscillation causes excess pore pressure (including oscillatory component and residual component) to develop at a generic point in the sediment bed. When the effective stresses between the individual grains vanish because of the residual pore pressure buildup, sediment liquefaction occurs and the sediment mixture acts as a fluid.

The value of the residual pore pressure responses strongly depends on the dynamic wave pressure acting on the surface of the sediment bed. Under the action of 6, 10, 14 cm wave loadings, the value of residual pore pressure was less than the effective stress, and then residual pore pressure dissipated quickly. The sediment surface has settled by an amount S (S=1–2 cm, Fig. 7a) at time t<410 min in the course of wave loadings (part of S stems from the erosion of surface sediments). Since only wave loads were simulated in this wave flume (no unidirectional currents), the re-suspension sediments were attributed to the reciprocating wave orbital velocities before the seabed liquefaction. The experiments of Guo et al. (2016) and Zhang et al. (2018b) were also conducted in the same wave flume using similar Huanghe River silts, to evaluate the contribution of seabed liquefaction/fluidization to sediment resuspension. The results indicate that the resuspension sediments before the seabed liquefaction is less than 50% of the total suspension under the model scales. In the present study, the results also indicated the amount of re-suspended sediments is limited before the seabed liquefaction, and only a thin high concentration layer formed the near-bed bottom. The vertical distribution of the SSC profile is shown in Fig. 8b$_1$ and Fig. 8b$_2$.

With the sediment liquefied, the interlocking of solid particles was loosed and translated fluid-like sediment. The water column and the liquefied sediment form a two-layer-fluid region (Z_L < 0 < H) (Fig. 8c$_2$). Following the onset of liquefaction, the liquefied sediment with a distinct "orbital motion" and the liquefied zone extends downwards. The range of BBL extended downward to the liquefaction front, meanwhile, the vertical distribution of re-

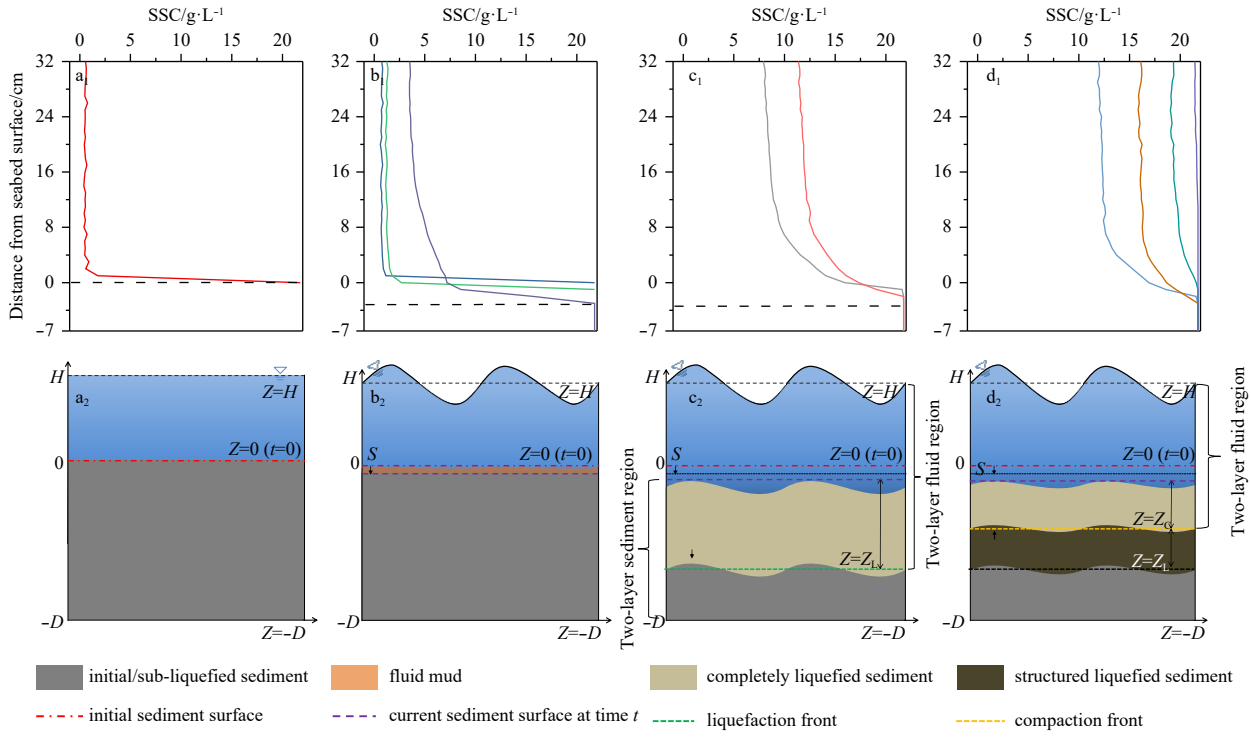

Fig. 8. The schematic mechanism for describing the progressive evolution of bottom boundary layer during the wave loadings (refer to) the wave-induced sediment oscillation.

suspended sediments in the water column expanded upward. As it has been referred before, it was liquefaction leading to the great increase of SSC. Zhang et al. (2018) pointed out the contribution of fluidization (the present authors called it "liquefaction") is attributed to two physical mechanisms: (1) an attenuation of the erosion resistance of liquefied sediments in surface layers due to the disappearing of original cohesion and the uplifting effect resulting from upward seepage flows, and (2) seepage pumping of fines from the interior to the surface of liquefied seabed.

During the progressive liquefaction process, the visual observations indicate that there are also two-layer-sediment region (Fig. 8c$_2$). One is the completely liquefied sediment with an "orbital motion", and the other is sub-liquefied sediment. Therefore, the behavior of the bed sediments changes from essentially liquid in the upper layer (as a part of the BBL) to essentially solid in the lower layer. Sumer et al. (2006) too described this phenomenon. The interface between the two-layer sediment region is called "liquefaction front". When the liquefaction front extended downward to maximum depth, a transition layer in the lowermost part of the liquefied zone start developing, and the compaction will start developing. Now, the interface between the two-layer sediment region is called "compaction front". The liquefied sediment in the transition layer was called the structured liquefied sediment with marked densification owing to the compaction during continued wave loading (Fig. 8c$_2$). The compaction front advanced upwards during the continued wave loading. Miyamoto et al. (2004) discussed the process of compaction with marked densification in liquefied sand during continued wave loading and attributed this phenomenon to shear-induced contracting of sand due to the wave loading. Xu et al. (2016) carried out similar flume experiments using similar Yellow River silts, the results showed that the penetration resistance of structured liquefied sediment was remarkably enhanced (Fig. 9). The range of BBL in sediments decreased as the completely liquefied sediment changed from essentially liquid to essentially solid with the compaction front advanced upwards. It is noted that the SSC of water column increased continuously (discussed later).

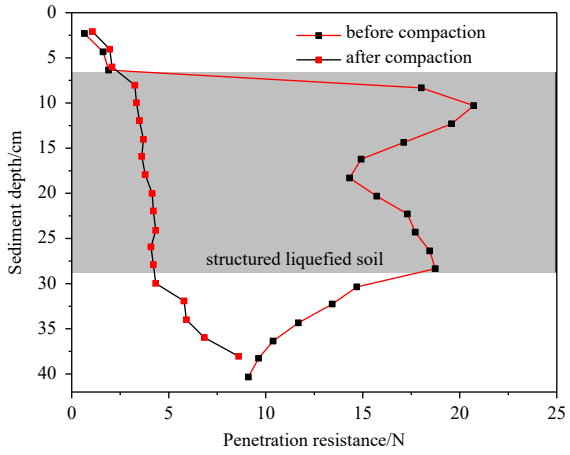

Fig. 9. The penetration resistance of structured liquefied sediment.

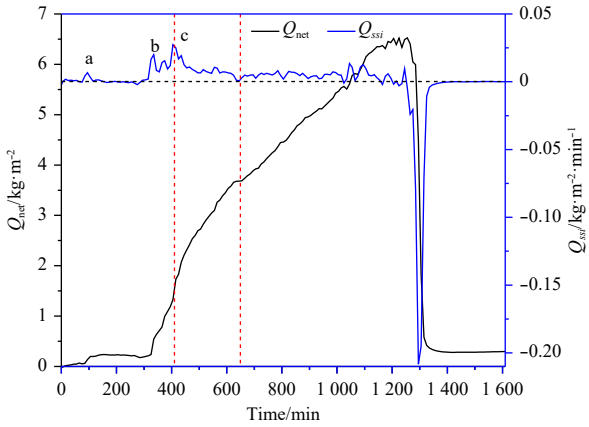

Fig. 10. The net re-suspended sediment (Q_{net}) per basal area water column and net re-suspended sediment increment (Q_{ssi}) which is the time derivative of Q_{net}.

4.2 *Variations in re-suspended sediment quantity*

The SSC in the water column is an important index for the variation of BBL. The silt sediments from the Yellow River Estuary have demonstrated fast initiation and re-suspension characteristics, and moderate wave energy could cause bottom silt resuspension (Wright et al., 1986). As mentioned previously, the sediments below water/sediment interface undergo erosion, liquefaction, and compaction owing to the water pressure above it, successively. The net re-suspended sediment (Q_{net}) per basal area water column and net re-suspended sediment increment (Q_{ssi}) which is the time derivative of Q_{net} are shown in Fig. 10. The initial re-suspended sediment increment generated in the erosion stage before the liquefaction was the re-suspended sediments from the surface sediment when the wave-induced shear stress reached the critical shear stress. There was a peak value of Q_{ssi} when the subsequent waves were switched on, such as a and b points in Fig. 10. With the buildup of excess pore pressure, an upward- directed pressure gradient is generated. This pressure gradient drove the water in the sediment upwards, which promoted the resuspension of sediments (Figs 10b–c). Zhang et al. (2017) putted forward a hypothesis of subbottom sediment pump action which argues that subsurface fine-grained sediments will be transported from the interior to the surface of a fluidized (or liquefied) seabed driven by the upward seepage flows resulting from the wave-induced nonuniform distribution of the pore pressure build up. The theoretical indicates that seabed liquefaction greatly promotes sediment resuspension. As shown in Fig. 10, another peak of Q_{ssi} occurred when the seabed liquefaction, and the Q_{net} continuously increased accompanying the reciprocating arc-shaped oscillation motion of part of the sediment bed. It can be explained using the conceptual model of sediment fluidization by Liu et al. (2013). During the compaction stage, the Q_{net} continuously increased, but the value of Q_{ssi} was smaller than which in the liquefaction stage.

5 Conclusions

The dynamics process of the Bottom Boundary Layer in silty seabed beneath progressive waves has been discussed. The principal conclusions obtained from the present study may be summarized as follows:

(1) The BBL in silty seabed is exposed to a progressive wave, goes through a number of different stages including compaction before liquefaction, sediment liquefaction, and compaction after liquefaction, which determines the range and thickness of BBL.

(2) With the introduction of waves, first, the sediment surface has settled by an amount S (S=1–2 cm) in the course of wave loadings with an insufficient accumulation of pore water pressure. And a thin high concentration layer formed the near-bed bottom.

(3) Once the liquefaction sets in, the completely liquefied sediment with an "orbital motion" and the sub-liquefied sediment

form a two-layer-sediment region. The range of BBL extends downwards with the liquefaction front and stopped at a certain depth, subsequently, develops upwards with the compaction process. Meanwhile, re-suspended sediments diffuse to the upper water column.

(4) Accumulation and dissipation of excess pore water pressure play an important role in the evolution of BBL and sediment re-suspension. With the buildup of excess pore pressure, an upward-directed pressure gradient is generated, which urges the subsurface fine-grained sediments transported from the interior to the surface.

(5) During the dynamics process of the Bottom Boundary Layer beneath progressive waves, the re-suspended sediment increment ranked as sediment liquefaction > erosion before liquefaction > compaction after liquefaction.

Acknowledgements

The authors thank Guohui Xu, Lei Guo, Xiaolei Liu for providing many helpful suggestions, Cui Kai and Shen Zezhong at the Ocean University of China for contributions to the laboratory analysis. The authors also appreciate the anonymous English editor's constructive comments, which greatly improved both the science and the quality of our original manuscript.

References

Bowden K F. 1978. Physical problems of the benthic boundary layer. Geophysical Surveys, 3(3): 255–296, doi: 10.1007/BF01449556

Bruens A. 2003. Entrainment mud suspensions [dissertation}. Delft, The Netherlands: Delft University of Technology.

Chang H K, Shih C J, Liu T J, et al. 2012. Curtain coating of dilute suspensions. Polymer Engineering and Science, 52(1): 1–11, doi: 10.1002/pen.22031

Guo Lei, Wen Mingzheng, Shan Hongxian, et al. 2016. Study on resuspension process of seabed sediment induced by wave. Marine Geology & Quaternary Geology (in Chinese), 36(5): 181–188

Hir P L, Bassoullet P, Jestin H. 2000. Application of the continuous modeling concept to simulate high-concentration suspended sediment in a macrotidal estuary. Proceedings in Marine Science, 3: 229–247, doi: 10.1016/S1568-2692(00)80124-2

Ingliss C C, Allen F H. 1957. The regimen of the Thamcs as affected by currents, salinities and river Row. Proceedings of the Institute of Civil Engineers, 7: 827–878, doi: 10.1680/iicep.1957.2705

Jeng D S. 2001. Mechanism of the wave-induced seabed instability in the vicinity of a breakwater: a review. Ocean Engineering, 28(5): 537–570, doi: 10.1016/S0029-8018(00)00013-5

Jeng D S. 2013. Porous Models for Wave-seabed Interactions. Berlin: Springer, 95–120

Jia Yonggang, Zhang Liping, Zhang Jiewen, et al. 2014. Effects of wave-induced seabed liquefaction on sediment re-suspension in the Yellow River Delta. Ocean Engineering, 89: 146–156, doi: 10.1016/j.oceaneng.2014.08.004

Kantha L H, Clayson C A, Moum J. 2000. Small scale processes in geophysical fluid flows. Physics Today, 54(10): 74–75

Kineke G C, Sternberg R W, Trowbridge J H, et al. 1996. Fluid-mud processes on the Amazon continental shelf. Continental Shelf Research, 16(5–6): 667–696, doi: 10.1016/0278-4343(95)00050-X

Krone R B. 1962. Flume studies of the transport of sediment in estuarial shoaling process. Berkeley: Hydraulic Engineering Laboratory and Sanitary Engineering Laboratory, University of California, 110.

Liu Xiaolei, Jia Yonggang, Zheng Jiewen, et al. 2013. Experimental evidence of wave-induced inhomogeneity in the strength of silty seabed sediments: Yellow River Delta, China. Ocean Engineering, 59: 120–128, doi: 10.1016/j.oceaneng.2012.12.003

Liu Xiaolei, Jia Yonggang, Zheng Jiewen, et al. 2016. An experimental investigation of wave-induced sediment responses in a natural silty seabed: New insights into seabed stratification. Sedimentology, 64(2): 508–529, doi: 10.1111/sed.12312

Lueck R. 2001. Turbulence in the benthic boundary layer. In: Steele J H, ed. Encyclopedia of Ocean Sciences. London: Elsevier Science Ltd, 265(1322): 3057–3063

McKee B A, Aller R C, Allison M A, et al. 2004. Transport and transformation of dissolved and particulate materials on continental margins influenced by major rivers: benthic boundary layer and seabed processes. Continental Shelf Research, 24(7–8): 899–926, doi: 10.1016/j.csr.2004.02.009

Miyamoto J, Sassa S, Sekiguchi H. 2004. Progressive solidification of a liquefied sand layer during continued wave loading. Géotechnique, 54(10): 617–629, doi: 10.1680/geot.2004.54.10.617

Mörz T, Karlik E A, Kreiter S, et al. 2007. An experimental setup for fluid venting in unconsolidated sediments: New insights to fluid mechanics and structures. Sedimentary Geology, 196(1–4): 251–267, doi: 10.1016/j.sedgeo.2006.07.006

Prior D B, Yang Z S, Bornhold B D, et al. 1986. The subaqueous delta of the modern huanghe (yellow river). Geo-Marine Letters, 6(2): 67–75, doi: 10.1007/BF02281642

Ross M A. 1988. Vertical structure of estuarine fine sediment suspensions [dissertation}. Gainesville, FL: University of Florida, 188

Sumer B M, Hatipoglu F, Fredsøe J. 2004. The cycle of soil behaviour during wave liquefaction. Book of Abstracts, Procedings of 29th International Conference on Coastal Engineering, ICCE. Lisbon: ICCE 2004 Organizing Committee, 171–171

Sumer B M, Hatipoglu F, Fredsøe J, et al. 2006. The sequence of sediment behaviour during wave-induced liquefaction. Sedimentology, 53(3): 611–629, doi: 10.1111/j.1365-3091.2006.00763.x

Sun Yongfu, Dong Lifeng, Song Yupeng. 2008. Analysis of characteristics and formation of disturbed soil on subaqueous delta of Yellow River. Rock and Soil Mechanics (in Chinese), 29(6): 1494–1499

Van Den Berg J H, Gelder V. 1993. Prediction of suspended bed material transport in flows over silt and very fine sand. Water Resources Research, 29(5): 1393–1404, doi: 10.1029/92WR02654

Wan Yuanyang, Roelvink D, Li Wehua, et al. 2014. Observation and modeling of the storm-induced fluid mud dynamics in a muddy-estuarine navigational channel. Geomorphology, 217: 23–36, doi: 10.1016/j.geomorph.2014.03.050

Wang Hu, Liu Hongjun, Zhang Minsheng. 2014. Pore pressure response of seabed in standing waves and its mechanism. Coastal Engineering, 91: 213–219, doi: 10.1016/j.coastaleng.2014.06.005

Wei Helong, Li Guangxue, Li Shaoquan. 1995. Prediction of sediment transport rate in the lower reaches of the yellow river. Marine Geology & Quaternary Geology (in Chinese), 15(4): 69–79

Wells J T. 1983. Dynamics of coastal fluid muds in low-, moderate-, high-tide-range environments. Canadian Journal of Fisheries and Aquatic Science, 40(S1): s130–s142, doi: 10.1139/f83-276

Winterwerp J C, Bruens A W, Gratiot N, et al. 2002. Dynamics of concentrated benthic suspension layers. Proceedings in Marine Science, 5: 41–55, doi: 10.1016/S1568-2692(02)80007-9

Wright L D, Yang Z S, Bornhold B D, et al. 1986. Hyperpycnal plumes and plume fronts over the huanghe (Yellow River) Delta front. Geo-Marine Letters, 6(2): 97–105, doi: 10.1007/BF02281645

Xu Guohui, Liu Zhiqin, Sun Yongfu, et al. 2016. Experimental characterization of storm liquefaction deposits sequences. Marine Geology, 382: 191–199, doi: 10.1016/j.margeo.2016.10.015

Xu Guohui, Wei Congcong, Sun Yongfu, et al. 2008. The engineering characteristics of shallow disturbed strata and analysis of their formation on the subaqueous Yellow River Delta. Marine Geology & Quaternary Geology (in Chinese), 28(6): 19–25

Zhang Shaotong, Jia Yonggang, Wen Mingzheng, et al. 2017. Vertical migration of fine-grained sediments from interior to surface of seabed driven by seepage flows-'sub-bottom sediment pump action'. Journal of Ocean University of China, 16(1): 15–24, doi: 10.1007/s11802-017-3042-0

Zhang Shaotong, Jia Yonggang, Zhang Yaqi, et al. 2018a. Influence of seepage flows on the erodibility of fluidized silty sediments: parameterization and mechanisms. Journal of Geophysical Research: Oceans, 123(5): 3307–3321, doi: 10.1002/2018JC013805

Zhang Shaotong, Jia Yonggang, Wang Zhenhao, et al. 2018b. Wave flume experiments on the contribution of seabed fluidization to sediment resuspension. Acta Oceanologica Sinica, 37(3): 1–8, doi: 10.1007/s13131-018-1195-3